TECHNICAL MEMORANDUM

459

The Impact of Moist Singular Vectors and Horizontal Resolution on Short-Range Limited-Area Ensemble Forecasts for two European Winter Storms

A. Walser[1], M. Arpagaus[1], M. Leutbecher and C. Appenzeller[1]

Research Department

[1]Swiss Federal Office of Meteorology and Climatology (MeteoSwiss), Zürich

Submitted to Monthly Weather Review

March 30, 2005

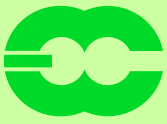

European Centre for Medium-Range Weather Forecasts
Europäisches Zentrum für mittelfristige Wettervorhersage
Centre européen pour les prévisions météorologiques à moyen terme

Series: ECMWF Technical Memoranda

A full list of ECMWF Publications can be found on our web site under:
http://www.ecmwf.int/publications/

Contact: library@ecmwf.int

European Centre for Medium-Range Weather Forecasts
Shinfield Park, Reading, RG2 9AX, England

Abstract

This paper studies the impact of different initial condition perturbation methods and horizontal resolutions on short-range limited-area ensemble predictions for two severe winter storms. The methodology consists of 51 member ensembles generated with the global ensemble prediction system (EPS) of the European Centre for Medium-Range Weather Forecasts which are downscaled with the nonhydrostatic limited-area model LM. The resolution dependency is studied by comparing 3 different limited-area ensembles: a) 80 km grid-spacing, b) 10 km grid-spacing, and c) 10 km grid-spacing with a topography coarse grained to 80 km resolution. The initial condition perturbations of the global ensembles are based on singular vectors (SVs), and the tendencies are not perturbed (i.e., no stochastic physics). Two configurations are considered for the initial condition perturbations: (i) the operational SV configuration: T42 truncation, 48-h optimization time, and dry tangent-linear model, and (ii) the "moist SV" configuration: T_L95 truncation, 24-h optimization time, and moist tangent-linear model.

LM ensembles are analyzed for the European winter storms Lothar and Martin, both occurring in December 1999, with particular attention paid to near-surface wind gusts. It is shown that forecasts using the moist SV configuration predict higher probabilities for strong wind gusts during the storm period compared to forecasts with the operational SV configuration. Similarly, the forecasts with increased horizontal resolution - even with coarse topography - lead to higher probabilities compared to the low resolution forecasts. Overall, the two case studies suggest that currently developed operational high-resolution limited-area EPSs have a great potential to improve early warnings for severe winter storms, particularly when the driving global EPS employs moist SVs.

1 Introduction

Probabilistic weather forecasting methodologies have been developed in order to take into account the chaotic behavior of the atmospheric synoptic-scale flow (see the reviews by Ehrendorfer, 1997; Palmer, 2000). Since 1992, global ensemble prediction systems (EPSs) based on multiple forecasts became operational at NMC (now NCEP; Toth and Kalnay, 1997) and at the European Centre for Medium-Range Weather Forecasts (ECMWF; Molteni et al., 1996). Currently this approach is mainly used for forecasting systems in the medium to longer time range, while short-range forecasting systems mostly rely on a deterministic approach. The latter choice may not generally be ideal, especially when considering forecasts of extreme weather events. These rare events populate the tails of the probability density function (PDF) of atmospheric states. Ensemble forecasts predict an estimate for the time evolution of the PDF and hence provide a basis for weather risk information. Investigating three storms occurring in Europe in December 1999, Buizza and Hollingsworth (2002) pointed out the benefit of the ECMWF EPS versus the ECMWF deterministic model. The ECMWF EPS uses singular vectors (SVs) to create optimally perturbed initial states (Buizza and Palmer, 1995). In a recent paper, Hoskins and Coutinho (2005) showed that SVs based on an extended physics package (see also later in section 2.2), referred to as moist SVs hereafter, are more relevant to severe cyclonic development than those currently used operationally at ECMWF.

However, current global EPSs use coarse resolutions and are limited in predicting appropriate PDFs for extreme weather events on a regional scale. Thus, in the last decade, studies have also been devoted to mesoscale predictability using limited-area ensembles (e.g., Stensrud et al., 2000; Walser et al., 2004a) and reported considerable improvements compared to global EPS forecasts, in particular for forecasting heavy precipitation (e.g., Frogner and Iversen, 2002; Marsigli et al., 2001). Motivated by these results, initiatives for operational high-resolution EPSs have emerged recently using various strategies, encompassing a multimodel ensemble including most of the European operational forecasts (Quiby and Denhard, 2003) and downscaling of several representative members selected from a global EPS with a limited-area model (Montani et al., 2003, see also later in section 4.3).

During the days after Christmas 1999, western Europe was hit by two very intense storms. The first storm, called Lothar[1], crossed Europe on 26 December and caused huge damages on buildings and forests in France, southern Germany, and Switzerland. In fact, it was one of the most devastating storms in Central Europe in the last decades. Detailed insights into the dynamical aspects of this storm are provided by Wernli et al. (2002). On 27/28 December, the second storm, Martin, passed over Europe causing heavy damages in central and southern France, northern Spain, and Corsica. Lothar and Martin caused economic losses of some 12 billion and 6 billion USD, respectively, and more than 80 casualties (Bresch et al., 2000). The purpose of this paper is to examine the impact of horizontal resolution and the use of moist SVs on high-resolution ensemble forecasts for these two intense extra-tropical cyclones. To this end, high-resolution ensemble simulations are performed to adapt the global-scale EPS of the ECMWF to the regional scale.

The paper is organized as follows: The relevant features of the limited-area model and the experimental setup are described in section 2. Section 3 presents the two investigated storm events and tests the models ability to simulate these storms, while section 4 compares the ensemble simulations with different model resolutions and different SV configurations. Finally, conclusions are presented in section 5.

2 Experimental set-up

2.1 The LM

The ensemble simulations presented in this study were conducted with the Lokal Modell version 3.9 (LM; see Doms and Schättler, 2002; Steppeler et al., 2003) of the Consortium for Small-scale Modelling (COSMO). The model is based on the compressible set of nonhydrostatic equations for flow in a moist atmosphere. The prognostic equations for momentum, pressure perturbation, temperature, water vapor and the condensed water species are discretized on a staggered Arakawa C grid (Arakawa, 1966) using the split-explicit time integration technique of Klemp and Wilhelmson (1978). In the vertical direction, a sigma-type coordinate based on base-state pressure is used implying time-independent terrain-following levels in the lower part and horizontal levels above $\sim$11 km. Rayleigh damping is used to absorb vertically propagating waves. The momentum, temperature, and pressure perturbation are relaxed to the interpolated fields of the global model between 11 km altitude and the model top at about 24 km.

The physical parameterization package of the LM is described by Doms et al. (2004). Short- and longwave radiation are parameterized by the Ritter and Geleyn (1992) scheme. Precipitation processes are represented by an extended version of the Kessler (1969) scheme including snow and cloud ice. Moist convection is parameterized by the mass flux scheme of Tiedtke (1989). The vertical turbulent diffusion is based on a prognostic equation for the turbulent kinetic energy (TKE) using a level 2.5 closure scheme (Raschendorfer, 2001). Over land (grid points with a land fraction larger than 50%) the soil model TERRA provides temperature and specific humidity of the ground using two soil layers.

A novel formulation for the wind gust diagnosis by Brasseur (2001) has been implemented in the LM version used in this study. This approach is based on the mean wind and the prognostic subgrid-scale turbulent kinetic energy and assumes that surface gusts result from air parcels at higher levels in the boundary layer which are transported to the near-surface layer by turbulent eddies.

[1] Also referred to as the 'French storm' or the '1999 Boxing Day low'

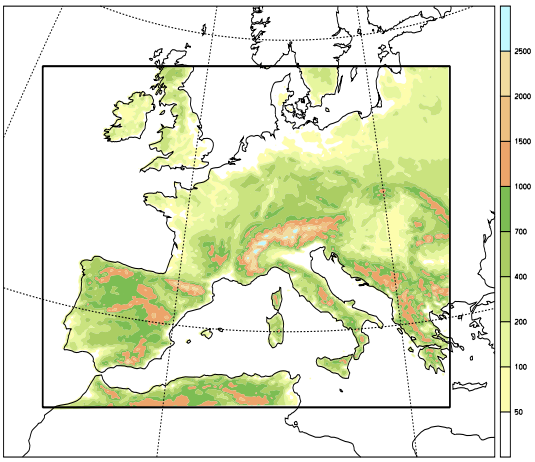

Figure 1: Computational domain of the limited-area ensemble simulations. The background field shows the LM model orography for 10 km grid-spacing.

2.2 LM ensemble experiments

Ensembles in this paper consists of 51 members (including an unperturbed control run). The initial and boundary conditions for the limited-area ensemble members are provided by global 51 member ensembles based on model cycle 26r3 of the ECMWF Integrated Forecast System (IFS). The global ensembles have T255 horizontal resolution and 40 vertical levels. The limited-area ensembles use the LM on a rotated spherical grid with a grid-spacing of $0.09^\circ \times 0.09^\circ$ (all such measures in this paper are latitude by longitude), equivalent to about 10 km between grid points, and 32 vertical levels. The LM integration area covers southern and central Europe as shown in Fig. 1. The lateral boundary conditions use a relaxation to the fields of the global model similar to the formulation discussed by Davies (1976).

Two different sets of initial perturbations are considered in the global ensembles. The first set is constructed from SVs computed with the operational configuration (see Buizza et al., 2001), the second set from so-called moist SVs. The latter are calculated with a more sophisticed version of the tangent-linear model (TLM) of the IFS using an extended linearized physics package (Mahfouf, 1999; Coutinho et al., 2004). In addition, the moist SVs are calculated with a horizontal resolution of T_L95 (triangular truncation at wave number 95 and a linear grid) rather than T42, and a 24-h optimization time (OT) rather than 48-h, which may result in a more reliable spread for shorter lead-times (i.e., days 2-3). As discussed in Coutinho et al. (2004), the inclusion of a large-scale condensation scheme in the TLM has the largest impact among the additional parameterizations of the extended physics package on the structure of the SVs and provides fast-growing perturbations that are not

Table 1: Set-up for the different LM ensembles.

Identification	IFS Perturbations	LM grid-spacing	LM orography	time step
HR-moist	moist SVs	0.09° x 0.09°	0.09° x 0.09°[1]	60 s
HR-opr	opr SVs	0.09° x 0.09°	0.09° x 0.09°[1]	60 s
HRCO-moist	moist SVs	0.09° x 0.09°	0.75° x 0.75°	60 s
HRCO-opr	opr SVs	0.09° x 0.09°	0.75° x 0.75°	60 s
LR-moist	moist SVs	0.75° x 0.75°	0.75° x 0.75°	300 s
LR-opr	opr SVs	0.75° x 0.75°	0.75° x 0.75°	300 s

[1]Smoothed with the Raymond (1988) filter using $\varepsilon = 0.1$ and $p = 5$.

included in the operational SVs. However, further work, beyond the scope of this paper, would be required to determine whether the impact due to the changed SV configuration can be attributed mostly to the representation of moist processes in the tangent-linear model as the work by Coutinho et al. (2004) indicates.

Six different LM ensemble configurations have been used in order to investigate the impact of moist SVs and horizontal resolution on limited-area ensemble forecasts (cf. Tab. 1). More specifically, in addition to the grid-spacing of about 10 km (experiments referred to as HR) ensembles are also computed with the grid-spacing of the ECMWF EPS of ∼80 km (referred to as LR) as well as with ∼10 km, but with the interpolated coarse topography of the ECMWF EPS (referred to as HRCO). These limited-area ensembles are driven with global ensembles using moist SVs (referred to as 'moist') and operational SVs (referred to as 'opr'), respectively. For all experiments, the stochastic simulation of model uncertainties (Buizza et al., 1999) is switched off.

2.3 LM analyses as proxy observations

The LM includes a nudging assimilation scheme which uses conventional observations to force the simulated atmospheric fields towards these observations (see Schraff and Hess, 2003). This scheme is used to derive LM analyses for the two winter storms with the same LM configuration as for the HR experiments. The analyses are used as proxy observations for the present study. The observations used for the assimilation are retrieved from the ECMWF Meteorological Archival and Retrieval System (MARS). They include surface observations (pressure, humidity, and 10 m wind), radio-soundings (wind, temperature, and humidity profiles) and aircraft observations (wind and temperature). Initial and lateral boundary conditions for the LM analyses are derived from the ERA-40 (T159L60) reanalysis (Simmons and Gibson, 2000).

3 Cases

In this section, we present an overview of the two winter storms considered and investigate the models ability to simulate the strong wind gusts reliably. To this end, two 72-h LM analyses, initialized on 24 and 26 December 1999 0000 UTC, respectively, are discussed with particular emphasis on simulated and observed sea level pressure (SLP) and wind gusts (one second averages).

While Lothar was a very small-scale secondary vortex moving extremely rapid, Martin was of a larger scale and crossed Europe somewhat slower. These characteristics are illustrated in Fig. 2 showing SLP of the LM analysis at the time when the analyzed core pressure attains its minimum. Additionally, the corresponding storm tracks are shown. Storm Lothar crossed Europe at about 49°N moving ∼2000 km in 20 hours while Martin passed over Europe at about 47° N moving ∼1900 km in 23 hours.

Figure 3a shows the time evolution of the minimum SLP in the center of storm Lothar as simulated in the LM analysis, and a comparison with values from the Deutscher Wetterdienst (DWD) derived from observations. The LM analysis highlights the explosive development of the storm (-22 hPa in 10 hours), even though it underestimates the minimum SLP by 5 hPa with a delay of about 2.5 hours. Otherwise, the LM analysis and the observations are very similar.

The intensification of cyclone Martin is exceptional, too (Fig. 3b). On 27 December 0700 UTC, the analyzed core SLP is 997 hPa. In the following 10 hours, the core SLP drops to 961 hPa showing an even more rapid pressure decrease than storm Lothar. The limited number of observations available for this case match those from the analysis fairly well.

The maximum wind gusts during both storm periods derived from the LM analysis are plotted in Fig. 4.

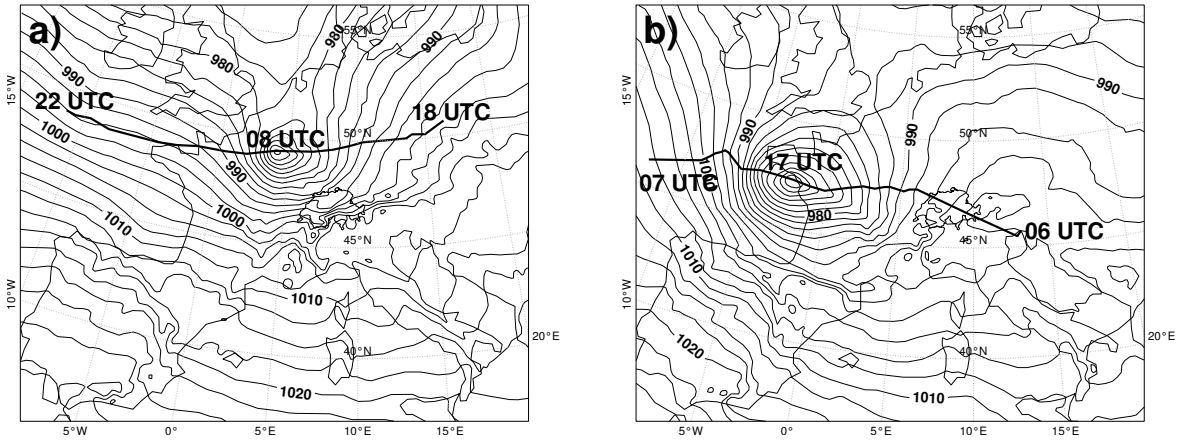

Figure 2: Overview of storm (a) Lothar and (b) Martin in terms of SLP (contours) and the storm track (bold line), both derived from an LM analysis (see text). Sea level pressure is shown for the time of simulated minimal core pressure, i.e., for (a) 26 Dec 1999 0800 UTC and (b) 27 Dec 1999 1700 UTC, respectively (cf. Fig. 3). Contours are smoothed and the contour interval is 2.5 hPa.

Storm Lothar caused gusts of more than 40 m/s in a 400 km broad band stretching from the Bay of Biscay into southern Germany. Gusts exceeded 50 m/s at some spots in the French Vosges and the Black Forest. Considering storm Martin, the region hit by gusts above 40 m/s is even larger and covered entire southwestern France, the Pyrenees, and some other elevated places in Spain as well as in Corsica. Moreover, the LM analysis shows a wide area with gusts exceeding 50 m/s over the Atlantic and the French coast around Bordeaux. Since wind gust observations were not archived in MARS before 2001, the following comparison of simulated and observed wind gusts is restricted to Switzerland: Figure 5 shows the observed maximum wind gusts at 59 stations of the Swiss automatic observation network below 2000 m a.s.l. for storm Lothar. In particular northern Switzerland and elevated places in the western mountain range reported wind gusts above 40 m/s (filled circles) or slightly below, whereas the regions south of the Alpine ridge were only weakly affected by the storm, consistent with the LM analysis. During storm Martin, Switzerland was less affected by strong wind gusts in agreement with the LM analysis. Below 2000 m a.s.l. they were in the range of about 20 m/s (eastern part) to 30 m/s (western part of the country).

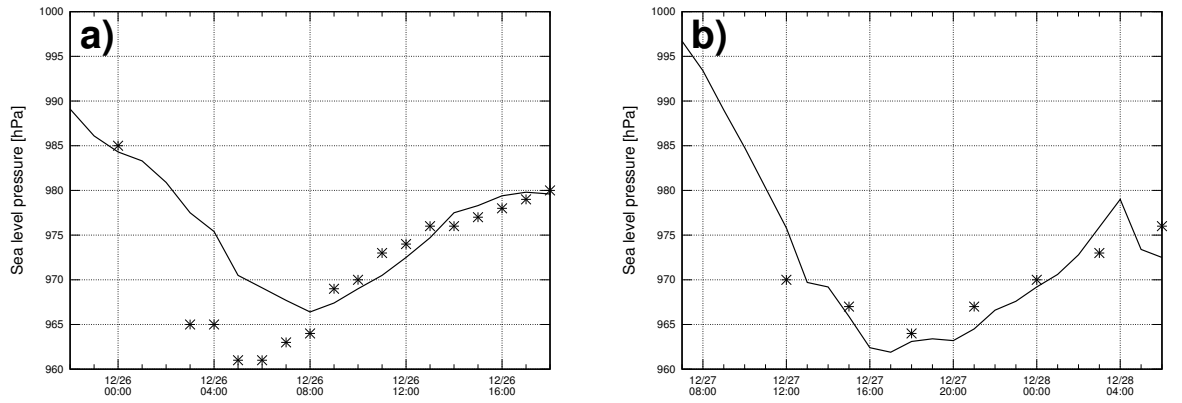

Figure 3: Time evolution of the minimum sea level pressure (hPa) in the center of the cyclone (a) Lothar and (b) Martin from the LM analysis (solid line) and observations (symbols; data from the Deutscher Wetterdienst (DWD)). Time is given on the abscissa (UTC).

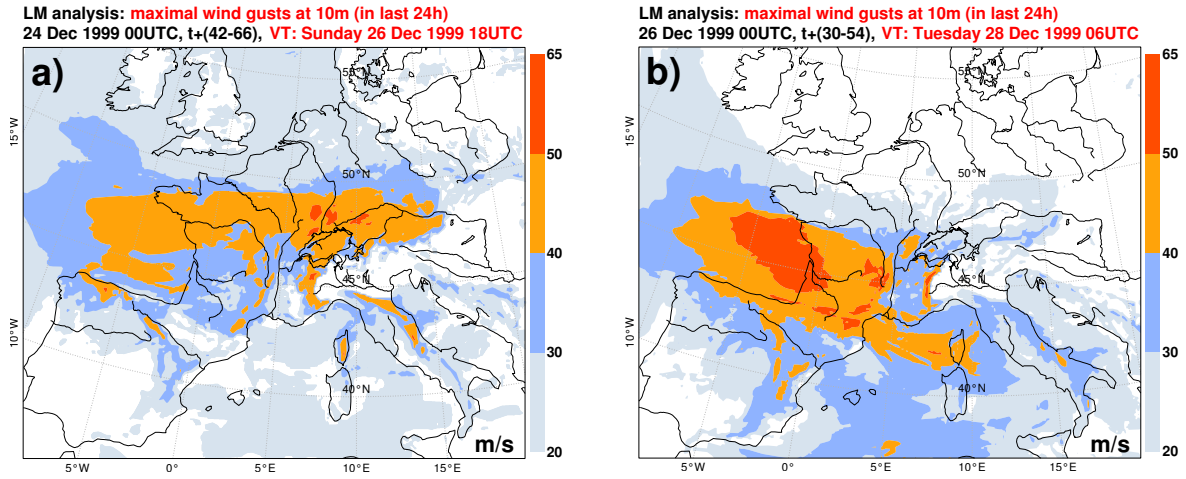

Figure 4: Wind gusts of LM analysis for (a) 26 Dec 1999 1800 UTC and (b) 28 Dec 1999 0600 UTC. The panels show maximum wind gusts (m/s) during the last 24 hours.

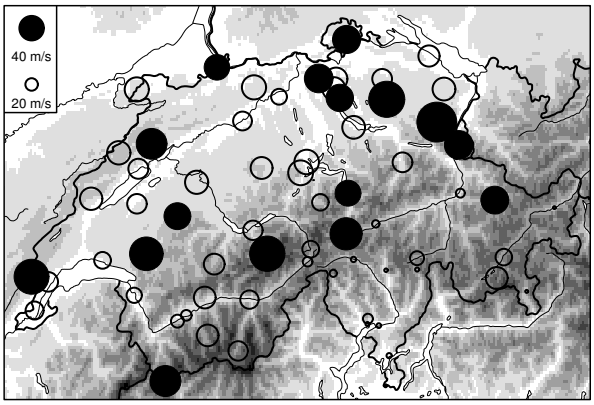

Figure 5: Observed maximum wind gusts between 25 Dec 1800 UTC and 26 Dec 1999 1800 UTC as size of centered circles (scale is indicated in the panel) for 59 stations below 2000 m a.s.l. of the automatic observation network of MeteoSwiss. Filled circles indicate wind gusts above 40 m/s.

In summary, the diagnosed wind gusts of the LM analyses – which do not use the observed wind gusts as input – match the Swiss observations fairly well, both in terms of absolute values and regional patterns. We conclude from this spatially limited validation, that the analyses seem to slightly overestimate the actual wind gusts rather than to underestimate them. For the following discussion of the results, regions showing maximum wind gusts above 40 m/s in the LM analysis will be referred to as *affected* regions for simplicity.

4 Results

In this section, we present the probabilistic wind gust forecasts and analyze the impact of horizontal resolution and initial conditions based on moist SVs on the forecasts for the two storms Lothar and Martin. In addition, a comparison with forecasts using smaller, operationally feasible ensemble sizes is discussed. The comparisons focus on SLP in the core of the cyclones and on the corresponding storm tracks as well as on maximum wind gusts. Particular attention is paid to the threshold of 40 m/s which is clearly exceeded in both storm events (cf.

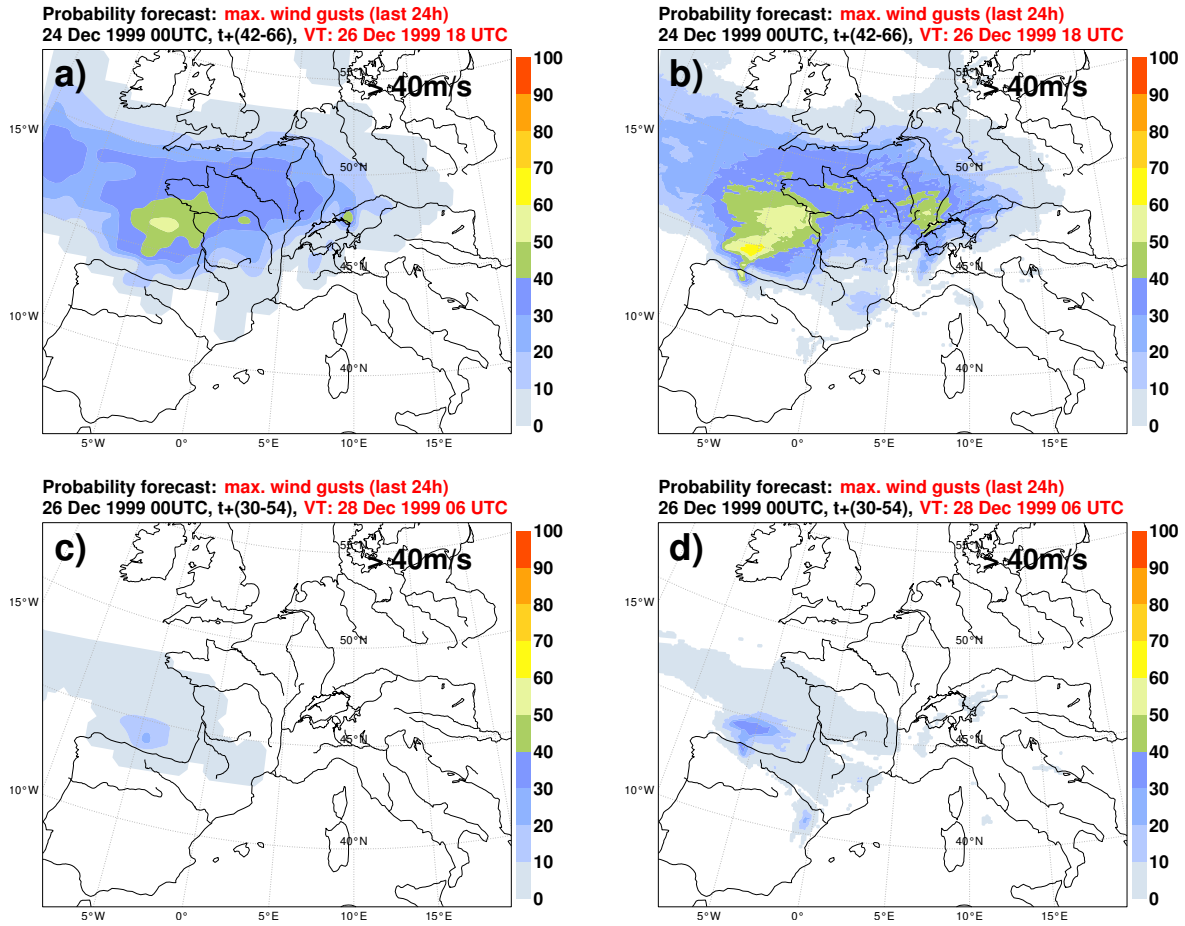

Figure 6: Probability forecast for maximum wind gusts above 40 m/s for storm (top) Lothar and (bottom) Martin, respectively, during the last 24 hours for (top) 26 Dec 1999 1800 UTC and (bottom) 28 Dec 1999 0600 UTC. The panels show the results for LM ensembles with (left) 80 km (LR-opr) and (right) 10 km horizontal grid-spacing but same topography (HRCO-opr), respectively.

Fig. 4) and corresponds to a threshold for which substantial damages have to be expected.

4.1 Impact of horizontal resolution

The impact of horizontal resolution on probabilistic wind gust forecasts for the two storm events is investigated by comparing the LR-opr and HRCO-opr experiments (see Table 1). Both experiments use the same coarse topography to exclude effects due to resolving more orographic details. We begin the discussion with storm Lothar for which probability maps for maximum wind gusts above 40 m/s are shown in Fig. 6 (top) for both setups. The high-resolution ensemble HRCO-opr exhibits higher probabilities and more fine-scale structures than the LR-opr ensembles. Looking at the regions in central Europe including the French Vosges, the Black Forest, and northern Switzerland, an increase in probabilities from 0-30% to 10-50% can be observed. Just as conspicuous is the increase in probabilities over the eastern Atlantic, where the region with probabilities above 40% is larger in the HRCO-opr ensemble.

The experiments for storm Martin reveal a similar impact due to increasing the horizontal resolution as seen for Lothar, but on a lower level of forecasted probabilities for maximum wind gusts above 40 m/s (Fig. 6, bottom).

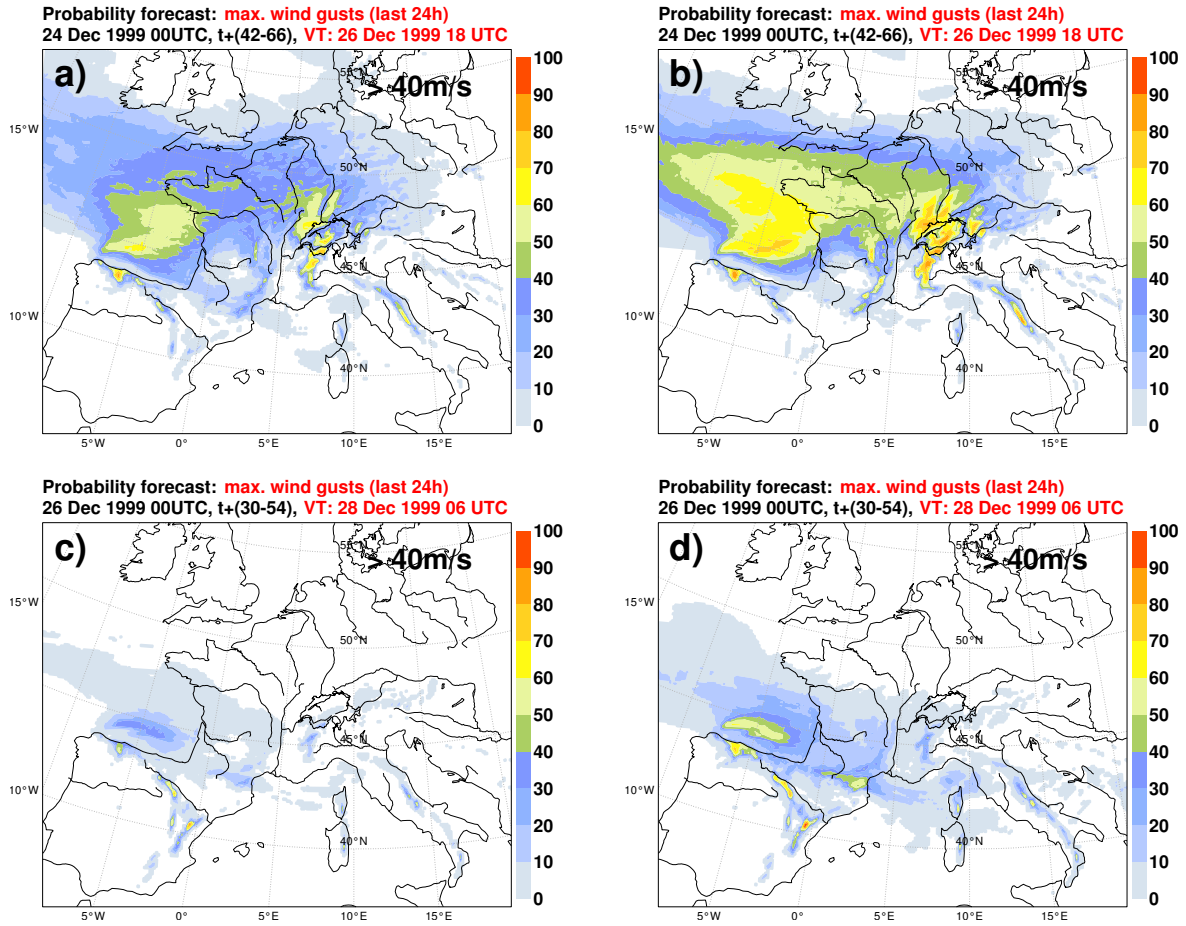

Figure 7: Same as Fig. 6, but for LM ensembles using (left) operational SVs (HR-opr) and (right) moist SVs (HR-moist), respectively, in the driving global ensemble.

The most obvious change between the LR-opr and the HRCO-opr ensembles is found over the Atlantic north of Spain. Also, the affected region in southern France with 0% predicted probability is smaller in the LR-opr ensemble.

In summary, the change in the horizontal grid-spacing from $0.09^\circ \times 0.09^\circ$ to $0.75^\circ \times 0.75^\circ$ has a significant impact on the probabilistic wind gust forecasts for both storms leading to moderate increases in the probabilities for wind gusts above 40 m/s. A comparison of the LR-moist and HRCO-moist experiments (not shown) confirms this result showing very similar changes in the probabilities. Hence, the processes relevant for the development of the storms can be simulated more accurately using a higher spatial resolution, i.e., using a limited-area EPS is beneficial as compared to a global EPS for this type of events.

4.2 Impact of moist singular vectors

This subsection describes the impact of using moist SVs instead of operational SVs for the determination of the initial conditions of the global ensemble. The global ensembles are downscaled with the LM using a 0.09° horizontal grid-spacing and topography (experiments HR-opr and HR-moist, respectively).

For storm Lothar, the use of moist SVs leads to a general increase in the probabilities for maximum wind gusts

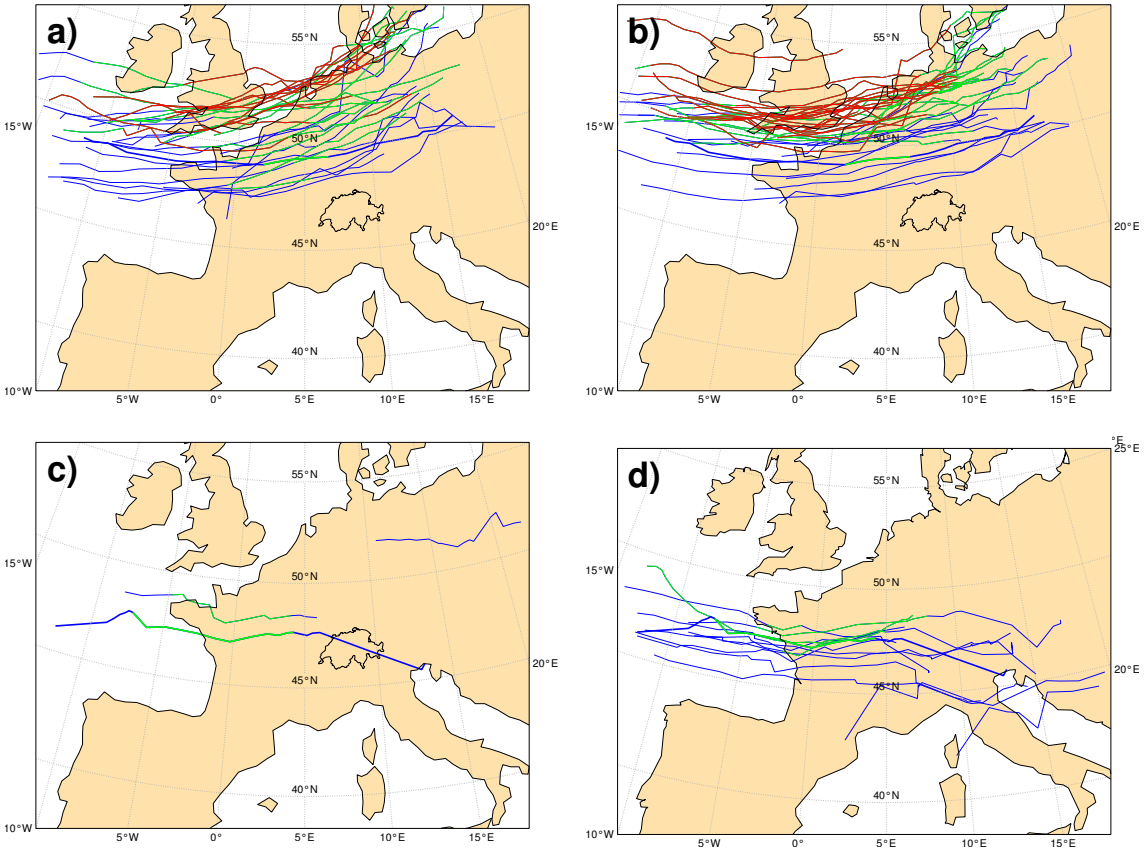

Figure 8: Predicted storm tracks (thin lines) and storm track of the LM analysis (bold line) between (top) 25 Dec 1999 1800 UTC, and 26 Dec 1999 1800 UTC and (bottom) 27 Dec 0600 UTC and 28 Dec 0600 UTC from (a, c) HR-opr and (b, d) HR-moist experiments. For each member, the track with the earliest and southernmost starting point of all tracks with a minimum sea level pressure (SLP) below 980 hPa and at least 1000 km west-east elongation is considered. SLPs below 970 and 960 hPa are indicated with green and red lines, respectively.

above 40 m/s in the regions affected by the storm (Fig. 7). The HR-moist experiment reveals values of 10 to 20% higher than in the HR-opr experiment and shows a west-east elongated band of probabilities above 40%, similar to the band with maximum wind gusts above 40 m/s in the LM analysis (cf. Fig. 4a).

For storm Martin, the HR-moist ensemble also yields higher probabilities than the HR-opr ensemble in regions affected by the storm. The increase is significant over the Atlantic north of Spain and in southern France. However, the absolute probabilities are still on a low level ranging from about 10% to 30% (but up to 60% over the Atlantic). On the other hand, probabilities for maximum wind gusts above 30 m/s (not shown) are considerable in the HR-moist (HR-opr) ensemble, reaching up to 80% (60%) in southern France.

In addition to looking at predicted probabilities, we now lock at storm tracks of individual ensemble members for both cases. To this end, all tracks within the respective 24-h period which have (i) a minimum SLP below 980 hPa and (ii) a west-east track elongation of at least 1000 km, are determined. Out of these, the track with the earliest and southernmost starting point is selected, i.e., at most one track per ensemble member. For the Lothar experiments, most of the predicted storm tracks are found north of the observed track with lower minimum SLP in the core (Fig. 8, cf. color coding). A comparison between both setups exhibits 36 members (out of a maximum of 51) with a storm track in the HR-moist and 32 members in the HR-opr ensemble. In addition, the HR-moist ensemble reveals more very intense cyclones with a SLP below 960 hPa (indicated as red lines),

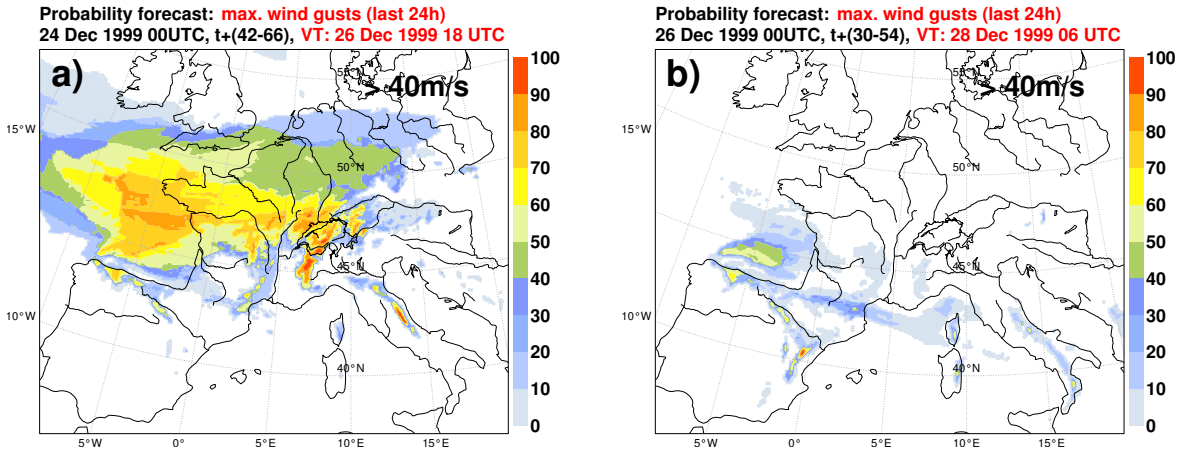

Figure 9: Same as Fig. 7 (b) and (d), but for an ensemble with 10 representative members (see text).

most of them at about 51° N.

The corresponding storm track analysis for storm Martin shows much larger differences between the HR-moist and HR-opr experiments. The former exhibits 10 tracks similar to the observed one (from a total of 12 tracks), while of the two tracks in the HR-opr only one shows some similarity to the observed track. Remarkable is the fact, that for these experiments almost all predicted cyclones are less intense than the observed one.

Overall, the use of moist SVs for the two storm events results in ensembles with a larger fraction of ensemble members predicting an intense storm leading to considerable increases in the probabilities for maximum wind gusts above 40 m/s. A comparison of the LR-moist and LR-opr as well as the HRCO-moist and HRCO-opr experiments, respectively, confirm this finding showing very similar changes in the probabilities (not shown). Hence, the moist SV configuration (moist tangent-linear model, higher spatial resolution, and shorter optimization time) provides initial condition perturbations which seem to be more relevant for the dynamics of the two storms than the perturbations based on the operational SV configuration.

4.3 Impact of ensemble size

In an operational environment, the downscaling of 51 global ensemble members is not feasible due to the large amount of required computer resources. In order to run a limited-area EPS in a quasi-operational setup, such as COSMO-LEPS (Montani et al., 2003; Walser et al., 2004b), an ensemble reduction technique where only a few representative members of the global ensemble are selected to drive limited-area integrations has been developed by ARPA-SIM, Bologna, Italy (Molteni et al., 2001; Marsigli et al., 2001). The ensemble reduction procedure is carried out by performing a multivariate hierarchical cluster analysis on the global ensemble members with a fixed number of clusters. This clustering is based on horizontal wind, humidity, and geopotential in the lower-to-middle troposphere (850, 700, and 500 hPa, respectively) for the full LM model domain. A representative member (RM) for each of the clusters is then defined by selecting the member with the minimum ratio between distances from the other members of the same cluster and distances from all the remaining members of the other clusters. These RMs then provide initial and boundary conditions for the limited-area integrations which are weighted according to the number of global ensemble members in the corresponding cluster.

For this study, subsamples of 5, 10, and 20 downscaled RMs have been derived using the clustering time steps +24h, +48h, and +72h. Ideally, a probabilistic forecast using RMs shows an identical forecast as the corresponding 51 member ensemble, since it aims to represent the entire ensemble. The results show that

forecasts using 10 and 20 RMs provide very similar probability forecasts for wind gusts, close to those for the 51 members, while forecasts using only 5 RMs clearly differ from the results of the full ensembles.

Figure 9 shows the 10 member forecasts for storm Lothar and Martin with the HR-moist setup. The probability patterns are quite similar to the corresponding patterns of the 51 member ensemble (cf. Figs. 7b, d), but shows somewhat different amplitudes. While for the Lothar ensemble the probabilities are clearly higher in the 10 member ensemble, they are somewhat lower for the Martin ensemble compared to the corresponding 51 member ensembles, respectively.

In summary, our comparison for the two selected storm events confirms the usefulness of such an ensemble reduction technique necessary for an operational limited-area EPS.

5 Conclusions

This paper studies the impact of different initial condition perturbation methods and horizontal resolution on short-range limited-area ensemble predictions for two severe winter storms. To this end, 51 member ensembles generated with the global ECMWF EPS are downscaled with the nonhydrostatic limited-area numerical weather prediction model LM for the two storms Lothar and Martin occurring in December 1999. The initial conditions in the global ensembles are based on two different configurations: the currently operational configuration and a 'moist SV' configuration. The limited-area LM ensembles are calculated with 10 km horizontal grid-spacing, as well as with 10 km horizontal grid-spacing but 80 km topography, and with 80 km horizontal grid-spacing for comparison. They are analyzed focusing on probabilistic wind gust predictions and on storm tracks of individual ensemble members.

While for Lothar a large fraction of the ensemble members suggests a storm over Europe, only a few members show a signal for Martin. It is shown that forecasts using moist SVs enhance the predicted probabilities for the observed strong wind gusts for both storms. This results from (i) a larger number of members with a pronounced storm track, and from (ii) typically more intense cyclones in the corresponding experiments. Similarly, the forecasts with increased horizontal resolution - even with coarse topography - lead to higher probabilities compared to the low resolution forecasts. In addition, it is shown that subsamples of at least 10 representative downscaled members according to the procedure of Marsigli et al. (2001) are able to produce forecasts similar to those using all ensemble members, even for such extreme events as Lothar and Martin.

Our study has some notable limitations. In particular, the results are based on only two cases which precludes to draw more general conclusions. Further, it is unknown whether the higher resolution or the moist SV configuration, both leading to higher probabilities for strong wind gusts in the investigated cases, would also lead to higher probabilities for non-events, i.e., to a higher false alarm rate. In addition, the wind gust formulation is far from being perfect and overestimates wind gusts substantially for another European storm (F. Schubiger, pers. comm.). Finally, further inspections, beyond the scope of this paper, have revealed that the moist SVs optimized for 24 hours lead to an underdispersive ensemble in the medium-range. The lack of spread in the medium-range appears to arise from the limited growth that the moist SVs exhibit beyond the optimization time of 24 hours. Work in progress examines whether a revision of the linearized physics package or a combination of SVs optimized for 24 hours and SVs optimized for 48 hours could improve the global ensemble at all forecast ranges.

In summary, our results suggest that high-resolution limited-area ensemble predictions driven by a global ensemble using initial condition perturbations based on SVs computed with a moist T_L95 tangent-linear model and optimized for 24 hours may have a greater potential to provide early warnings for intense extra-tropical cyclones than coarser resolution global ensembles using SVs computed with a dry T42 tangent-linear model

and optimized over 48 hours. Further work will be required to determine whether the moist SV configuration also improves short-range limited-area ensemble forecasts for other types of extreme events such as heavy precipitation.

Acknowledgments

The authors are indebted to Tiziana Paccagnella and her research group at the Regional Hydro-Meteorological Service of Emilia-Romagna, Bologna, Italy (ARPA-SIM), for providing access to and support for the COSMO-LEPS clustering code and the postprocessing tools to derive probabilistic model output. We are grateful to Tim Palmer for supporting this study. The research has been funded through the NCCR-Climate program sponsored by the Swiss National Science Foundation (grant 5005-65755).

References

Arakawa, A., 1966: Computational design for long term numerical integrations of the equations of fluid motion. *J. Comp. Phys*, **1**, 119–143.

Brasseur, O., 2001: Development and application of a physical approach to estimating wind gusts. *Mon. Wea. Rev.*, **129**, 5–25.

Bresch, D. N., M. Bisping, and G. Lemcke, 2000: Storm over Europe: An underestimated risk, swiss Re Publishing, available at Swiss Re, CH-8022 Zurich, and from http://www.swissre.com.

Buizza, R., and A. Hollingsworth, 2002: Storm prediction over Europe using the ECMWF ensemble prediction system. *Meteorol. Appl.*, **9**, 289–305.

Buizza, R., and T. N. Palmer, 1995: The singular-vector structure of the atmospheric general circulation. *J. Atmos. Sci.*, **52**, 1434–1456.

Buizza, R., M. Miller, and T. N. Palmer, 1999: Stochastic simulation of model uncertainties. *Quart. J. Roy. Meteor. Soc.*, **125**, 2887–2908.

Buizza, R., D. S. Richardson, and T. N. Palmer, 2001: The new 80-km high-resolution ECMWF EPS, ECMWF Newsletter No. 90.

Coutinho, M. M., B. J. Hoskins, and R. Buizza, 2004: The influence of physical processes on extratropical singular vectors. *J. Atmos. Sci.*, **61**, 195–209.

Davies, H., 1976: A lateral boundary formulation for multi-level prediction models. *Quart. J. Roy. Meteor. Soc.*, **102**, 405–418.

Doms, G., and U. Schättler, 2002: A description of the nonhydrostatic regional model LM, available from http://cosmo-model.org.

Doms, G., J. Förstner, E. Heise, H.-J. Herzog, M. Raschendorfer, R. Schrodin, T. Reinhardt, and G. Vogel, 2004: A description of the nonhydrostatic regional model LM. Part II: Physical parameterization, available from http://cosmo-model.org.

Ehrendorfer, M., 1997: Predicting the uncertainty of numerical weather forecasts: A review. *Meteor. Z.*, **6**, 147–183.

Frogner, I.-L., and T. Iversen, 2002: High-resolution limited-area ensemble predictions based on low-resolution targeted singular vectors. *Quart. J. Roy. Meteor. Soc.*, **128**, 1321–1341.

Hoskins, B. J., and M. M. Coutinho, 2005: Moist singular vectors and the predictability of some high impact European cyclones. *Quart. J. Roy. Meteor. Soc.*, **131**, 581–601.

Kessler, E., 1969: On the distribution and continuity of water substance in the atmospheric circulations. *Meteor. Monogr.*, vol. 10, Amer. Meteor. Soc.

Klemp, J., and R. Wilhelmson, 1978: The simulation of three-dimensional convective storm dynamics. *J. Atmos. Sci.*, **53**, 1070–1096.

Mahfouf, J.-F., 1999: Influence of physical processes on the tangent linear-approximation. *Tellus*, **51A**, 147–166.

Marsigli, C., A. Montani, F. Nerozzi, T. Paccagnella, S. Tibaldi, F. Molteni, and R. Buizza, 2001: A strategy for high-resolution ensemble prediction. Part II: Limited-area experiments in four Alpine flood events. *Quart. J. Roy. Meteor. Soc.*, **127**, 2095–2115.

Molteni, F., R. Buizza, T. N. Palmer, and T. Petroliagis, 1996: The ECMWF ensemble prediction system: Methodology and validation. *Quart. J. Roy. Meteor. Soc.*, **122**, 73–119.

Molteni, F., R. Buizza, C. Marsigli, A. Montani, F. Nerozzi, and T. Paccagnella, 2001: A strategy for high-resolution ensemble prediction. Part I: Definition of representative members and global-model experiments. *Quart. J. Roy. Meteor. Soc.*, **127**, 2069–2094.

Montani, A., M. Capaldo, D. Cesari, C. Marsigli, U. Modigliani, F. Nerozzi, T. Paccagnella, P. Patruno, and T. S., 2003: Operational limited-area ensemble forecasts based on the Lokal Modell, ECMWF Newsletter No. 98.

Palmer, T. N., 2000: Predicting uncertainty in forecasts of weather and climate. *Rep. Prog. Phys.*, **63**, 71–116.

Quiby, J., and M. Denhard, 2003: SRNWP-DWD poor-man ensemble prediction system: The PEPS project, EUMETNET Newsletter, No. 8, available from http://www.eumetnet.eu.org.

Raschendorfer, M., 2001: The new turbulence parameterization of LM, COSMO Newsletter, No. 1, available from http://www.cosmo-model.org.

Raymond, W. H., 1988: High-order low-pass implicit tangent filters for use in finite area calculations. *Mon. Wea. Rev.*, **116**, 2132–2141.

Ritter, B., and J.-F. Geleyn, 1992: A comprehensive radiation scheme for numerical weather prediction models with potential applications in climate simulations. *Mon. Wea. Rev.*, **120**, 303–325.

Schraff, C., and R. Hess, 2003: A description of the nonhydrostatic regional model LM. Part III: Data assimilation, available from http://cosmo-model.org.

Simmons, A. J., and J. K. Gibson, 2000: The ERA-40 project plan, ERA-40 Project Report Series, No. 1, ECMWF, Reading, available from http://www.ecmwf.int.

Stensrud, D. J., J. W. Bao, and T. T. Warner, 2000: Using initial conditions and model physics in short-range ensemble simulations of mesoscale convective systems. *Mon. Wea. Rev.*, **128**, 2077–2107.

Steppeler, J., G. Doms, U. Schättler, H.-W. Bitzer, A. Gassmann, U. Damrath, and G. Gregoric, 2003: Meso-gamma scale forecasts using the nonhydrostatic model LM. *Meteorol. Atmos. Phys.*, **82**, 75–96.

Tiedtke, M., 1989: A comprehensive mass flux scheme for cumulus parameterization in large scale models. *Mon. Wea. Rev.*, **117**, 1779–1799.

Toth, Z., and E. Kalnay, 1997: Ensemble forecasting at NCEP and the breeding method. *Mon. Wea. Rev.*, **125**, 3297–3319.

Walser, A., D. Lüthi, and C. Schär, 2004a: Predictability of precipitation in a cloud-resolving model. *Mon. Wea. Rev.*, **132**, 560–577.

Walser, A., M. W. Rotach, M. Arpagaus, C. Appenzeller, C. Marsigli, and A. Montani, 2004b: A limited-area ensemble prediction system, preprints International workshop on Timely Warnings of heavy precipitation episodes and flash floods, Ljubljana, 21-22 October, 5pp (published by the Slowenian Meteorological Society).

Wernli, H., S. Dirren, M. Liniger, and M. Zillig, 2002: Dynamical aspects of the life-cycle of the winter storm 'Lothar' (24-26 December 1999). *Quart. J. Roy. Meteor. Soc.*, **128**, 405–430.